

40

60

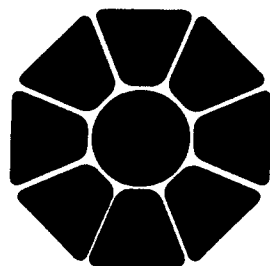
CERN LIBRARIES, GENEVA



SCAN-9601147

CLNS 95/1370

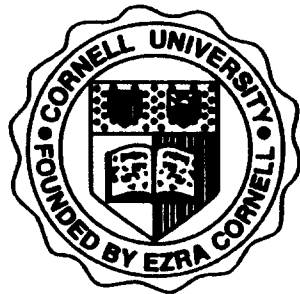
CLEO 95-19



CLEO

**CALTECH UC-SAN DIEGO UC-SANTA BARBARA CARLETON COLORADO
CORNELL FLORIDA HARVARD HAWAII ILLINOIS ITHACA KANSAS MCGILL
MINNESOTA SUNY-ALBANY OHIO STATE OKLAHOMA PURDUE ROCHESTER
SOUTHERN-METHODIST SLAC SYRACUSE VANDERBILT VIRGINIA TECH**

Tau Decays into Three Charged Leptons and Two Neutrinos



PREPRINT LIBRARY
Floyd R. Newman Laboratory
of Nuclear Studies
Cornell University
Ithaca, N.Y. 14853 U.S.A.

Tau decays into three charged leptons and two neutrinos.

M.S. Alam,¹ I.J. Kim,¹ Z. Ling,¹ A.H. Mahmood,¹ J.J. O'Neill,¹ H. Severini,¹ C.R. Sun,¹ S. Timm,¹ F. Wappler,¹ J.E. Duboscq,² R. Fulton,² D. Fujino,² K.K. Gan,² K. Honscheid,² H. Kagan,² R. Kass,² J. Lee,² M. Sung,² C. White,² R. Wanke,² A. Wolf,² M.M. Zoeller,² X. Fu,³ B. Nemati,³ S.J. Richichi,³ W.R. Ross,³ P. Skubic,³ M. Wood,³ M. Bishai,⁴ J. Fast,⁴ E. Gerndt,⁴ J.W. Hinson,⁴ T. Miao,⁴ D.H. Miller,⁴ M. Modesitt,⁴ E.I. Shibata,⁴ I.P.J. Shipsey,⁴ P.N. Wang,⁴ L. Gibbons,⁵ S.D. Johnson,⁵ Y. Kwon,⁵ S. Roberts,⁵ E.H. Thorndike,⁵ C.P. Jessop,⁶ K. Lingel,⁶ H. Marsiske,⁶ M.L. Perl,⁶ S.F. Schaffner,⁶ R. Wang,⁶ T.E. Coan,⁷ J. Dominick,⁷ V. Fadeyev,⁷ I. Korolkov,⁷ M. Lambrecht,⁷ S. Sanghera,⁷ V. Shelkov,⁷ R. Stroynowski,⁷ I. Volobouev,⁷ G. Wei,⁷ M. Artuso,⁸ A. Efimov,⁸ M. Gao,⁸ M. Goldberg,⁸ D. He,⁸ N. Horwitz,⁸ S. Kopp,⁸ G.C. Moneti,⁸ R. Mountain,⁸ Y. Mukhin,⁸ S. Playfer,⁸ T. Skwarnicki,⁸ S. Stone,⁸ X. Xing,⁸ J. Bartelt,⁹ S.E. Csorna,⁹ V. Jain,⁹ S. Marka,⁹ D. Gibaut,¹⁰ K. Kinoshita,¹⁰ P. Pomianowski,¹⁰ S. Schrenk,¹⁰ B. Barish,¹¹ M. Chadha,¹¹ S. Chan,¹¹ G. Eigen,¹¹ J.S. Miller,¹¹ C. O'Grady,¹¹ M. Schmidtler,¹¹ J. Urheim,¹¹ A.J. Weinstein,¹¹ F. Würthwein,¹¹ D.M. Asner,¹² M. Athanas,¹² D.W. Bliss,¹² W.S. Brower,¹² G. Masek,¹² H.P. Paar,¹² J. Gronberg,¹³ C.M. Korte,¹³ R. Kutschke,¹³ S. Menary,¹³ R.J. Morrison,¹³ S. Nakanishi,¹³ H.N. Nelson,¹³ T.K. Nelson,¹³ C. Qiao,¹³ J.D. Richman,¹³ D. Roberts,¹³ A. Ryd,¹³ H. Tajima,¹³ M.S. Witherell,¹³ R. Balest,¹⁴ K. Cho,¹⁴ W.T. Ford,¹⁴ M. Lohner,¹⁴ H. Park,¹⁴ P. Rankin,¹⁴ J. Roy,¹⁴ J.G. Smith,¹⁴ J.P. Alexander,¹⁵ C. Bebek,¹⁵ B.E. Berger,¹⁵ K. Berkelman,¹⁵ K. Bloom,¹⁵ D.G. Cassel,¹⁵ H.A. Cho,¹⁵ D.M. Coffman,¹⁵ D.S. Crowcroft,¹⁵ M. Dickson,¹⁵ P.S. Drell,¹⁵ D.J. Dumas,¹⁵ R. Ehrlich,¹⁵ R. Elia,¹⁵ P. Gaidarev,¹⁵ R.S. Galik,¹⁵ B. Gittelmann,¹⁵ S.W. Gray,¹⁵ D.L. Hartill,¹⁵ B.K. Heltsley,¹⁵ C.D. Jones,¹⁵ S.L. Jones,¹⁵ J. Kandaswamy,¹⁵ N. Katayama,¹⁵ P.C. Kim,¹⁵ D.L. Kreinick,¹⁵ T. Lee,¹⁵ Y. Liu,¹⁵ G.S. Ludwig,¹⁵ J. Masui,¹⁵ J. Mevissen,¹⁵ N.B. Mistry,¹⁵ C.R. Ng,¹⁵ E. Nordberg,¹⁵ J.R. Patterson,¹⁵ D. Peterson,¹⁵ D. Riley,¹⁵ A. Soffer,¹⁵ C. Ward,¹⁵ P. Avery,¹⁶ A. Freyberger,¹⁶ C. Prescott,¹⁶ S. Yang,¹⁶ J. Yelton,¹⁶ G. Brandenburg,¹⁷ R.A. Briere,¹⁷ D. Cinabro,¹⁷ T. Liu,¹⁷ M. Saulnier,¹⁷ R. Wilson,¹⁷ H. Yamamoto,¹⁷ T. E. Browder,¹⁸ F. Li,¹⁸ J. L. Rodriguez,¹⁸ T. Bergfeld,¹⁹ B.I. Eisenstein,¹⁹ J. Ernst,¹⁹ G.E. Gladding,¹⁹ G.D. Gollin,¹⁹ M. Palmer,¹⁹ M. Selen,¹⁹ J.J. Thaler,¹⁹ K.W. Edwards,²⁰ K.W. McLean,²⁰ M. Ogg,²⁰ A. Bellerive,²¹ D.I. Britton,²¹ R. Janicek,²¹ D.B. MacFarlane,²¹ P.M. Patel,²¹ B. Spaan,²¹ A.J. Sadoff,²² R. Ammar,²³ P. Baringer,²³ A. Bean,²³ D. Besson,²³ D. Coppage,²³ N. Coptay,²³ R. Davis,²³ N. Hancock,²³ S. Kotov,²³ I. Kravchenko,²³ N. Kwak,²³ Y. Kubota,²⁴ M. Lattery,²⁴ J.K. Nelson,²⁴ S. Patton,²⁴ R. Poling,²⁴ T. Riehle,²⁴ and V. Savinov²⁴

(CLEO Collaboration)

¹State University of New York at Albany, Albany, New York 12222
²Ohio State University, Columbus, Ohio, 43210
³University of Oklahoma, Norman, Oklahoma 73019
⁴Purdue University, West Lafayette, Indiana 47907
⁵University of Rochester, Rochester, New York 14627
⁶Stanford Linear Accelerator Center, Stanford University, Stanford, California, 94309
⁷Southern Methodist University, Dallas, Texas 75275
⁸Syracuse University, Syracuse, New York 13244
⁹Vanderbilt University, Nashville, Tennessee 37235
¹⁰Virginia Polytechnic Institute and State University, Blacksburg, Virginia, 24061
¹¹California Institute of Technology, Pasadena, California 91125
¹²University of California, San Diego, La Jolla, California 92093
¹³University of California, Santa Barbara, California 93106
¹⁴University of Colorado, Boulder, Colorado 80309-0390
¹⁵Cornell University, Ithaca, New York 14853
¹⁶University of Florida, Gainesville, Florida 32611
¹⁷Harvard University, Cambridge, Massachusetts 02138
¹⁸University of Hawaii at Manoa, Honolulu, HI 96822
¹⁹University of Illinois, Champaign-Urbana, Illinois, 61801
²⁰Carleton University, Ottawa, Ontario K1S 5B6 and the Institute of Particle Physics, Canada
²¹McGill University, Montréal, Québec H3A 2T8 and the Institute of Particle Physics, Canada
²²Ithaca College, Ithaca, New York 14850
²³University of Kansas, Lawrence, Kansas 66045
²⁴University of Minnesota, Minneapolis, Minnesota 55455

Abstract

We have searched for the radiative leptonic tau decays $\tau \rightarrow ee^+e^- \nu_\tau \nu_e$ and $\tau \rightarrow \mu e^+e^- \nu_\tau \nu_\mu$ using 3.60 fb⁻¹ of data collected by the CLEO-II experiment at CESR. We present a first observation of the $\tau \rightarrow ee^+e^- \nu_\tau \nu_e$ process. For this channel we measure the branching fraction $B(\tau \rightarrow ee^+e^- \nu_\tau \nu_e) = (2.8 \pm 1.4 \pm 0.4) \times 10^{-5}$. An upper limit is established for the second channel: $B(\tau \rightarrow \mu e^+e^- \nu_\tau \nu_\mu) < 3.6 \times 10^{-5}$ at 90% CL. Both results are consistent with the rates expected from Standard Model predictions.

PACS numbers: 13.35.Dx

Tau decays into three charged leptons and two neutrinos are allowed processes in the Standard Model. They proceed via emission of a virtual photon with subsequent internal conversion into a pair of electrons or muons. Two Feynman diagrams provide the dominant contribution to the decay rate. They are shown in Fig. 1 for the $\tau^- \rightarrow \mu^- e^+ e^- \nu_\tau \bar{\nu}_\mu$ decay. The contribution of a third diagram, with a virtual photon emitted from the W boson, is heavily suppressed by the W propagator. For tau decays with two identical charged leptons in the final state, two additional exchange diagrams are involved. Branching fractions for these processes have been recently calculated by Dicus and Vega [1] and are listed in Table I. The branching fractions for tau decays with a virtual photon conversion into two muons, $\tau \rightarrow e\mu^+\mu^-\nu_\tau\nu_e$ and $\tau \rightarrow \mu\mu^+\mu^-\nu_\tau\nu_\mu$, are expected to be at the level of 10^{-7} , too small to be observed in existing data. On the other hand, the branching fractions for $\tau \rightarrow ee^+e^-\nu_\tau\nu_e$ and $\tau \rightarrow \mu e^+e^-\nu_\tau\nu_\mu$ are expected to be at the level of 10^{-5} which is comparable to the sensitivity reached in a recent search for neutrinoless tau decays into three charged particles [2]. In this Letter, we report on a follow-up study in which we have searched for these two decays.

The data used in this analysis were collected with the CLEO-II detector at the Cornell Electron Storage Ring (CESR), in which tau leptons are produced in pairs in e^+e^- collisions. Our study uses information from a 67-layer tracking system which also provides specific ionization measurements, time-of-flight scintillation counters and a 7800-crystal CsI calorimeter. These elements are inside a 1.5 T superconducting solenoidal magnet whose iron yoke also serves as a hadron absorber for a muon identification system. A detailed description of the apparatus can be found in Ref. [3]. About 60% of the events were obtained at the $\Upsilon(4S)$ resonance ($\sqrt{s} \simeq 10.59$ GeV) while the rest were obtained at energies approximately 60 MeV below the resonance. The data correspond to an integrated luminosity of about 3.60 fb^{-1} and the number of produced tau pairs, $N_{\tau\tau}$, is $(3.28 \pm 0.05) \times 10^6$.

A Monte Carlo event generator is needed in order to design the event selection procedure and to estimate the detector acceptance. We performed the calculation of the relevant matrix elements using the symbolic manipulation program FORM [4] and produced formulas in a format suitable for the Monte Carlo simulation. No tau polarization effects or higher order radiative corrections were taken into account. To check our generator, we used it to calculate the branching fraction for the known five lepton decay of the muon, $\mu \rightarrow eee\nu_\mu\nu_e$. The result, listed in Table I, is consistent with the previous calculation of Dicus and Vega and also with an earlier estimate $B(\mu \rightarrow eee\nu_\mu\nu_e) = (3.54 \pm 0.09) \times 10^{-5}$ by Bardin *et al.* [5]. It also agrees well with the experimental measurement $B(\mu \rightarrow eee\nu_\mu\nu_e) = (3.4 \pm 0.4) \times 10^{-5}$ by the SINDRUM collaboration [6]. For tau decays our branching fraction estimates are 6-7% higher than those of Dicus and Vega. The calculated branching fractions correspond to about 137 $\tau \rightarrow \mu e^+e^-\nu_\tau\nu_\mu$ and 292 $\tau \rightarrow ee^+e^-\nu_\tau\nu_e$ decays in our data sample. To study the kinematical properties of such events, we have generated 100,000 $\tau \rightarrow \mu e^+e^-\nu_\tau\nu_\mu$ and 60,000 $\tau \rightarrow ee^+e^-\nu_\tau\nu_e$ Monte Carlo decays. The KORALB/TAUOLA program package [7] was used to simulate the tau-pair production and the decay of the other tau in the event. Detector signals were simulated by the standard CLEO-II simulation program [8].

Fig. 2 illustrates momentum distributions for electrons from $\tau \rightarrow ee^+e^-\nu_\tau\nu_e$ decays. This plot reveals an intrinsic difficulty of detecting such tau decays: the electron spectrum is soft and peaks at very low momenta where there is a high probability for electron absorption in the beam pipe or for a mismeasurement of its trajectory and a misidentification. In the $\tau \rightarrow \mu e^+e^-\nu_\tau\nu_\mu$ channel the momentum distributions for both electrons and positrons are

similar to that shown as a dashed line in Fig. 2, while the corresponding muon distribution is much harder.

To extract from our data tau decays into three charged leptons and two neutrinos, we search for events where one tau decays into a single charged particle (1-prong decay) and the other tau decays into three charged particles (3-prong decay). The 3-prong decay is the signal candidate and the 1-prong decay is an allowed tau decay with one charged particle, zero or more photons and at least one neutrino in the final state. For each candidate event we require four well-reconstructed charged particle tracks with zero total charge. At CLEO-II center-of-mass energies, each tau lepton has sufficient boost to render its daughter particles well-separated from those of the other tau, so we select candidate events in a 1-vs-3 topology in which the most isolated track is separated by at least 90 degrees from all other tracks. We also reject events with photons with energy larger than $E > 60$ MeV on the 3-prong side.

Substantial background suppression comes from lepton identification on the 3-prong side. In the $\tau \rightarrow \mu e^+e^-\nu_\tau\nu_\mu$ channel we require a muon candidate with momentum less than 2.2 GeV/c to pass through at least 3 hadronic absorption lengths of iron and through at least 5 absorption lengths if its momentum is greater than 2.2 GeV/c. For such muon candidates, the energy deposited in the CsI calorimeter, E_c , must be compatible with that expected for a minimum ionizing particle: $0.1 \text{ GeV} < E_c < 0.5 \text{ GeV}$. We also require that the charge of the muon candidate is opposite to that of the 1-prong track. For electron identification, we rely mostly on specific ionization measurements in the drift chamber. We require that the electron candidate specific ionization differs from the expected value by less than 3 standard deviations, σ . If there is a time-of-flight measurement we require that it is compatible with the electron hypothesis within 3σ , and if the electron candidate reaches the CsI calorimeter we require that the ratio of the E_c to the electron momentum, p_e , is less than 1.1. This last requirement helps reject events where there is an undetected photon on the 3-prong side due to the overlap of its calorimeter energy deposit with an energy deposit from one of the electron candidates. In addition, the electron candidates with transverse momentum larger than 0.3 GeV/c and within the high resolution region of the calorimeter (*i.e.*, the angle between the track and the beam axis is greater than 45°) are required to have $E_c/p_e > 0.8$. The same E_c/p_e condition must be satisfied for all electron candidates with $p_e > 1.5$ GeV/c. For the $\tau \rightarrow ee^+e^-\nu_\tau\nu_e$ channel at least one electron candidate is required to have $E_c/p_e > 0.8$. In order to suppress a strong $e^+e^- \rightarrow e^+e^+e^-$ background we also require that in this channel the 1-prong particle is not consistent with being an electron. It must either pass through three absorption lengths of a muon filter or it must be within the high resolution region of the calorimeter, have transverse momentum larger than 0.3 GeV/c and have $E_c/p < 0.7$. The radiative muon pair background $e^+e^- \rightarrow \mu^+\mu^-e^+e^-$ in the $\tau \rightarrow \mu e^+e^-\nu_\tau\nu_\mu$ channel is reduced by the requirement that the 1-prong particle is not identified as a muon.

The main sources of background left after the lepton identification are: low multiplicity $e^+e^- \rightarrow q\bar{q}$ events, 2-photon processes, radiative Bhabha, μ -pairs and radiative leptonic decays $\tau \rightarrow l\nu_\tau\nu_l\gamma$ (l stands for e or μ) with subsequent $\gamma \rightarrow e^+e^-$ conversion in the detector material, tau decays into three hadrons and a neutrino where all hadrons are misidentified as leptons, and finally tau decays into $\rho\nu_\tau$ with subsequent $\rho \rightarrow \pi\pi^0$, $\pi^0 \rightarrow e^+e^-\gamma$ decays, where the γ escapes detection and the π is misidentified as a lepton.

In order to suppress a non-tau background, we require undetected neutrinos be present by selecting events with large missing energy, $E_{\text{miss}} > 1.5$ GeV, and a large value of total transverse momentum of the charged particles with respect to the beam direction, $p_t > 150$ MeV/c. The $\tau \rightarrow 3h\nu_\tau$ decays contribute to the background in our analysis due to a rather large branching fraction, about 8.4% [9], and a few percent probability for pions to fake leptons. To suppress this background, we estimate the probability that all electron candidates in the event are pions using the specific ionization measurements. We define the quantities:

$$\kappa_2 = \frac{P_{e^+P_{e^-}}}{P_{e^+P_{e^-}} + P_{\pi^+P_{\pi^-}}}, \quad \kappa_3 = \frac{P_e P_{e^+P_{e^-}}}{P_e P_{e^+P_{e^-}} + P_{\pi^+P_{\pi^-}}}$$

for the $\tau \rightarrow \mu e^+ e^- \nu_\tau \nu_\mu$ and $\tau \rightarrow ee^+ e^- \nu_\tau \nu_e$ channels respectively, where $P_e = (2\pi)^{-1/2} \exp(-\sigma_e^2/2)$ and $P_\pi = (2\pi)^{-1/2} \exp(-\sigma_\pi^2/2)$. Here, σ_e and σ_π are the numbers of standard deviations of measured specific ionization from that expected for an electron and a pion. κ_2 and κ_3 characterize the purity of the sample from a contamination with events with pions faking electrons. We require κ_2 and κ_3 to be greater than 0.97.

We check for photon conversions in our data sample by reconstructing a possible conversion point. At such point, the e^+ and e^- tracks should be parallel in the transverse plane perpendicular to the beam axis. We require that the distance from this point to the beam is less than 2 cm. This suppresses photon conversions because the closest distance where the photons can convert in the detector material is 3.5 cm from the beam axis (beam pipe radius). In the $\tau \rightarrow ee^+ e^- \nu_\tau \nu_e$ channel this requirement must be satisfied for both e^+e^- combinations.

In the $\tau \rightarrow \mu e^+ e^- \nu_\tau \nu_\mu$ and $\tau \rightarrow ee^+ e^- \nu_\tau \nu_e$ processes the invariant mass of the three charged leptons tends to be small and thus their tracks in the detector are nearly parallel. This feature provides the possibility of differentiating these decays from the $\tau \rightarrow \rho\nu_\tau, \rho \rightarrow \pi\pi^0, \pi^0 \rightarrow e^+e^-\gamma$ process where the γ escapes detection and the π is misidentified as a lepton. The distribution of the sum of the cosines of the angles ϑ_{ij} between the 3-prong tracks is shown in Fig. 3 for the data, signal Monte Carlo events and a sample of generic tau Monte Carlo events. We compare the distributions for the signal and generic tau Monte Carlo events and require $\sum_{i<j} \cos \vartheta_{ij} > 2.93$ for both channels.

The signal efficiency, ϵ , after application of all the selection requirements and accounting for tau pair tagging, is estimated from the Monte Carlo simulation to be $2.7 \pm 0.1\%$ for the $\tau \rightarrow ee^+ e^- \nu_\tau \nu_e$ channel and $1.9 \pm 0.1\%$ for the $\tau \rightarrow \mu e^+ e^- \nu_\tau \nu_\mu$ channel (statistical errors only). The very soft electron momentum spectrum is the main reason for such low efficiencies. With these estimates, our Standard Model calculations predict $7.8 \tau \rightarrow ee^+ e^- \nu_\tau \nu_e$ and $2.6 \tau \rightarrow \mu e^+ e^- \nu_\tau \nu_\mu$ remaining events on average. In the data, five events satisfy all selection criteria in the $\tau \rightarrow ee^+ e^- \nu_\tau \nu_e$ channel and one event in the $\tau \rightarrow \mu e^+ e^- \nu_\tau \nu_\mu$ channel. Distributions of several kinematic variables for both the signal Monte Carlo and the selected data events are shown in Fig. 4 for the $\tau \rightarrow ee^+ e^- \nu_\tau \nu_e$ channel. They indicate that the five remaining events in this channel are kinematically consistent with tau decays into three electrons and two neutrinos.

The remaining background from other tau decays is estimated by applying the above selection criteria to a sample of generic tau Monte Carlo events which does not include the signal channels and corresponds to an integrated luminosity of 10.2 fb^{-1} (about 2.8 times

larger than the data). No generic tau Monte Carlo events are accepted in either of the two channels. Thus, we estimate the background contribution from other tau decays to be less than 0.4 events at 68% confidence level (CL). No events satisfied our selection criteria from a sample of $6.1 \times 10^6 e^+e^- \rightarrow B\bar{B}$ and 1.4×10^7 continuum ($e^+e^- \rightarrow q\bar{q}$, $q = u, d, s$ and c) Monte Carlo events in either of the two channels. These samples are larger than the expected number of events in the data by factors of 2.6 and 1.2 respectively. Kinematic properties of the $B\bar{B}$ and continuum events are very dissimilar to those of the signal, and we conclude that these backgrounds are negligible. We expect no $e^+e^- \rightarrow e^+e^-e^+e^-$ background in the $\tau \rightarrow ee^+ e^- \nu_\tau \nu_e$ channel after requiring the 1-prong track not to be an electron. We checked this conclusion by looking at specific ionization measurements of the 1-prong tracks. These measurements favor the pion hypothesis over the electron one in all five remaining events. In addition, three of those events have a pair of photons on the 1-prong side with invariant mass compatible with that of a π^0 .

The main systematic errors in this study arise from uncertainties in our knowledge of the lepton identification efficiency and slow track reconstruction efficiency. Combined together, they are estimated to give an overall systematic error of 15%. We assume that the background rate in the $\tau \rightarrow ee^+ e^- \nu_\tau \nu_e$ channel is not larger than 0.4 events and calculate the branching fraction as

$$B(\tau \rightarrow ee^+ e^- \nu_\tau \nu_e) = (2.8 \pm 1.4 \pm 0.4) \times 10^{-5},$$

where the first error shows 68% confidence level bounds taking into account statistical fluctuations and possible background contamination. The obtained result is consistent at 23% confidence level with our calculated value of 4.46×10^{-5} .

Though one event is observed in the $\tau \rightarrow \mu e^+ e^- \nu_\tau \nu_\mu$ channel and its kinematical parameters are compatible with those of the expected signal, we are not able to make a reliable estimate of the corresponding branching fraction. Instead, we calculate an upper limit on this branching fraction as $3.89/(2\epsilon N_{\tau\tau})$ at 90% CL. As previously, we assign a systematic error of 15% to this result and increase the branching fraction limit by this amount. The resulting upper limit is

$$B(\tau \rightarrow \mu e^+ e^- \nu_\tau \nu_\mu) < 3.6 \times 10^{-5} \quad \text{at 90\% CL.}$$

The obtained limit is consistent with our theoretical calculation $B(\tau \rightarrow \mu e^+ e^- \nu_\tau \nu_\mu) = 2.09 \times 10^{-5}$.

We gratefully acknowledge the effort of the CESR staff in providing us with excellent luminosity and running conditions. This work was supported by the National Science Foundation, the U.S. Department of Energy, the Heisenberg Foundation, the Alexander von Humboldt Stiftung, the Natural Sciences and Engineering Research Council of Canada, and the A.P. Sloan Foundation.

REFERENCES

- [1] D.A. Dicus and R. Vega, Phys. Lett. B **338**, 341 (1994).
- [2] J. Bartelt *et al.*, Phys. Rev. Lett. **73**, 1890 (1994).
- [3] Y. Kubota *et al.*, Nucl. Instrum. Methods Phys. Res., Sect. A **320**, 66 (1992).
- [4] J.A.M. Vermaseren, The Symbolic Manipulation Program FORM, KEK-TH-326, Mar. 1992 (*unpublished*).
- [5] D.Yu. Bardin, Ts.G. Istatkov and G.B. Mitsel'makher, Sov. J. Nucl. Phys. **15**, 161 (1972).
- [6] W. Bertl *et al.*, Nuclear Physics B **260**, 1 (1985).
- [7] S. Jadach and Z. Was, Comput. Phys. Commun. **64**, 267 (1991); S. Jadach *et al.*, Comput. Phys. Commun. **76**, 361 (1993).
- [8] Detector simulation is based on the GEANT software package: R. Brun *et al.*, GEANT version 3.15, CERN DD/EE/84-1.
- [9] Particle Data Group, L. Montanet *et al.*, Phys. Rev. D **50**, 1403 (1994).

TABLES

TABLE I. Calculated τ and μ branching fractions. Errors given here are due to inaccuracies in numerical integration only.

Channel	Dicus & Vega	Our calculation
$\tau \rightarrow eee\nu_\tau\nu_e$	$(4.15 \pm 0.06) \times 10^{-5}$	$(4.457 \pm 0.006) \times 10^{-5}$
$\tau \rightarrow \mu ee\nu_\tau\nu_\mu$	$(1.97 \pm 0.02) \times 10^{-5}$	$(2.089 \pm 0.003) \times 10^{-5}$
$\tau \rightarrow e\mu\mu\nu_\tau\nu_e$	$(1.257 \pm 0.003) \times 10^{-7}$	$(1.347 \pm 0.002) \times 10^{-7}$
$\tau \rightarrow \mu\mu\mu\nu_\tau\nu_\mu$	$(1.190 \pm 0.002) \times 10^{-7}$	$(1.276 \pm 0.004) \times 10^{-7}$
$\mu \rightarrow eee\nu_\mu\nu_e$	$(3.60 \pm 0.02) \times 10^{-5}$	$(3.605 \pm 0.005) \times 10^{-5}$

FIGURES

FIG. 1. Feynman diagrams for the $\tau^- \rightarrow \mu^- e^+ e^- \nu_\tau \bar{\nu}_\mu$ process.

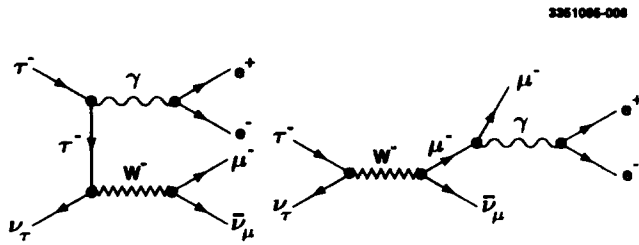


FIG. 2. Simulated momentum distributions for electrons (solid line, two entries per event) and positrons (dashed line) from $\tau^- \rightarrow e^- e^+ e^- \nu_\tau \bar{\nu}_e$ decays, in the laboratory system. The number of electrons, N_e , is normalized to unity in each histogram.

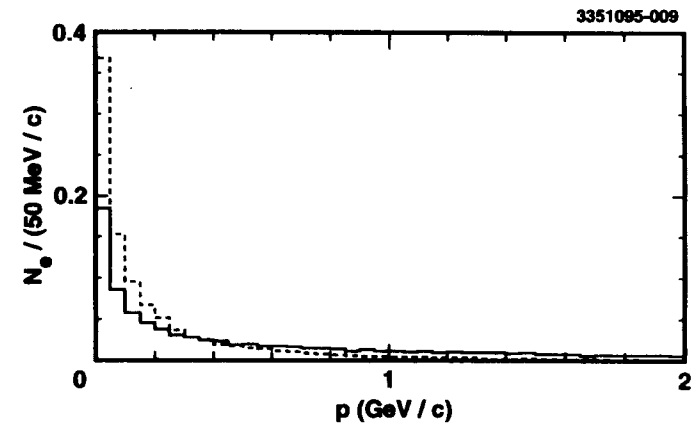


FIG. 3. Sum of cosines of the angles ϑ_{ij} between the 3-prong side tracks for the data (black circles), signal Monte Carlo (solid line) and generic tau Monte Carlo sample (dashed line) for the two channels studied. The signal Monte Carlo histograms are normalized to Standard Model theoretical predictions. The generic tau Monte Carlo histograms are normalized to the data luminosity. In this analysis we require $\sum_{i<j} \cos \vartheta_{ij} > 2.93$ for both channels.

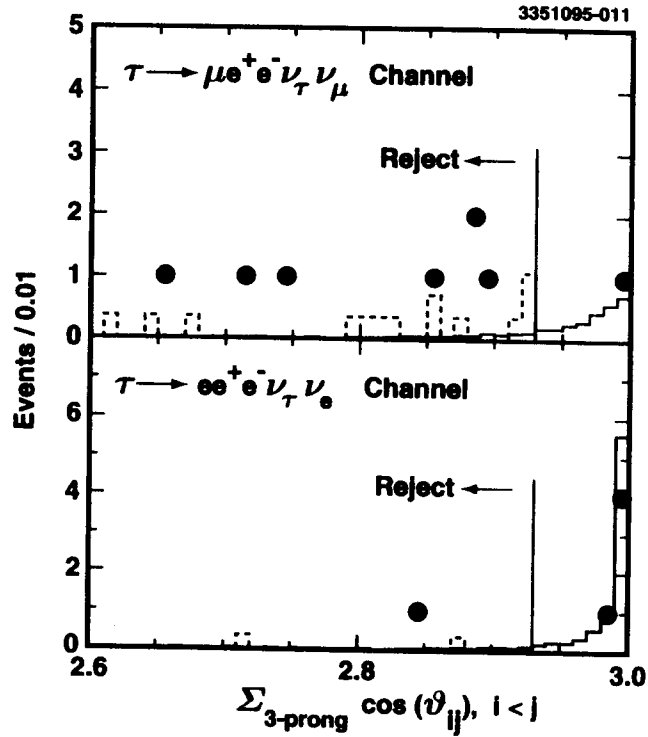


FIG. 4. Comparison of the kinematical distributions of the $\tau \rightarrow ee^+e^-\nu_\tau\nu_e$ Monte Carlo (solid line) and the data (shaded histogram) for events passing all selection requirements: a) the e^+e^- invariant mass averaged over two possible combinations, $M_{e^+e^-}$, b) the 3-prong invariant mass, $M_{3\text{-prong}}$, and c) the momentum of the electron on the 3-prong side with the charge opposite to that of the parent tau, P_{opp} . The normalization of the plots is arbitrary.

